Originally published 9 January 2014; revised 7 February 2014

www.sciencemag.org/content/full/343/6170/529/DC1

Supplementary Materials for

Marine Tubeworm Metamorphosis Induced by Arrays of Bacterial Phage Tail-like Structures

Nicholas J. Shikuma, Martin Pilhofer, Gregor L. Weiss, Michael G. Hadfield,*
Grant J. Jensen,* Dianne K. Newman*

*Corresponding author. E-mail: hadfield@hawaii.edu (M.J.H.); jensen@caltech.edu (G.J.J.); dkn@caltech.edu (D.K.N.)

Published 9 January 2014 on *Science* Express
Published 31 January 2014, *Science* **343**, 529 (2014)
DOI: 10.1126/science.1246794

This PDF file includes

Other Supplementary Material for this manuscript includes the following:
(available at www.sciencemag.org/cgi/content/full/science.1246794/DC1)

Revision 7 February 2014:
These corrections were provided for print. One text correction was made, and the figures were reprocessed because the conversion of the figures did not work properly.

Materials and Methods

Bacterial strains, plasmids and culture conditions.

Strains and plasmids used in this study are listed in Table S3. *P. luteoviolacea* was grown aerobically at 25˚C or 30˚C and *Escherichia coli* was grown aerobically at 37˚C. *E. coli* was cultured in lysogeny broth (LB) containing 10 g tryptone, 5 g yeast extract, 10 g NaCl per liter. *P. luteoviolacea* was cultured in artificial seawater tryptone (ASWT), natural seawater tryptone (NSWT) or Bacto Marine Broth Medium 2216 (Difco) medium. ASWT contained 2.5 g tryptone, 1.5 g yeast extract, 1.5 ml glycerol and 35.95 g Instant Ocean (United Pet Group, Blacksburg, VA) artificial seawater salts per liter. NSWT medium contained 1L 0.22 μm filtered natural seawater, 2.5 g tryptone, 1.5 g yeast extract, 1.5 ml glycerol. 2216 was prepared as described by the manufacturer. Agar medium contained 15 g granulated agar and 100 g sucrose per liter when necessary. Kanamycin and streptomycin were used at concentrations of 50 μg/ml for *E. coli* and 200 μg/ml for *P. luteoviolacea*.

Recombinant DNA techniques.

DNA manipulations were carried out using standard molecular techniques (*30*). DNA modification enzymes were obtained from New England Biolabs. Polymerase Chain Reactions (PCRs) were carried out with primers purchased from Integrated DNA Technologies and Kapa HiFi HotStart ReadyMix (Kapa Biosystems). Primers used in the present study were purchased from Integrated DNA Technologies Inc. (Coralville, IA) and primer sequences are listed in Table S4. Plasmid sequences were verified by DNA sequencing by Retrogen Inc. (San Diego, CA).

Generation of in-frame deletion mutants and translational fusion strains.

Plasmids for in-frame deletions were constructed by amplifying approximately 1000 bp long DNA fragments upstream and downstream of each target gene by PCR. The fragments were cloned into pCVD443 at the BamHI, SacI or SphI restriction sites using Gibson Assembly Master Mix (New England Biolabs Inc., Ipswich, MA) according to the manufacturer's instructions. Deletion plasmids generated harbor an approximately 2000 bp fragment of DNA that contains an in-frame deletion of the gene with the exception of the first and last 4 to 12 codons. The plasmid for generating strains with the *macB-sfgfp* fusion inserted into the native chromosomal locus was constructed by amplifying approximately 1000 bp long DNA fragments flanking the chromosomal insertion site. The two fragments were fused to a DNA fragment encoding sfGFP and cloned into pCVD443 at the BamHI and SphI restriction sites. DNA of *macB* was fused to DNA encoding for sfGFP separated by a DNA linker encoding 3XAla 3XGly. The accuracy of each plasmid constructed was verified by DNA sequencing. Conjugation of deletion or protein fusion plasmids was carried out between *E. coli* SM10 λ*pir* and various *P. luteoviolacea* strains. Exconjugants were selected on SWT agar containing kanamycin and streptomycin. A second *sacB*-mediated recombination event was selected for on SWT agar supplemented with sucrose. Isolates containing the desired in-frame deletion or translational fusion were identified by PCR with primers that flank the chromosomal DNA region of interest.

Culture of *Hydroides elegans* and metamorphosis assays.
Specimens of *H. elegans* were obtained from Marina Del Rey, CA, and maintained in culture at Caltech. Gametes were spawned and embryos maintained as previously described (*6*) except Instant Ocean artificial seawater (ASW) (35.95 g/L) was used in place of natural seawater. *Isochrysis galbana,* Tahitian strain, was provided as food for adults and larvae. Assays for induction of metamorphosis by various strains of bacteria were performed as previously described (*8*). Briefly, bacterial strains were grown overnight aerobically in ASWT or NSWT media. Cells were pelleted at 4000 g for 2 min, washed with sterile ASW, and cell density was adjusted to approximately 10^7-10^8 cells/ml. Cell suspensions were aliquoted into 24-well or 96-well plates and incubated for 1 hour to allow bacterial surface attachment. After incubation, unattached bacteria were removed by gently rinsing the wells three times with sterile ASW. Approximately 30-50 competent (6 to 7-day-old) larvae of *H. elegans* were added to each well and incubated at room temperature for 24 h. After incubation, the total numbers of larvae and metamorphosed juveniles were counted and a percent metamorphosis was calculated. At least 4 technical replicates of each treatment were used in all assays performed and at least three biological replicates were performed on separate occasions.

Western blot analysis.
P. luteoviolacea strains were cultured overnight (14-16 h) in ASWT media and 1 ml was centrifuged for 20 min at 15,000 g at 4˚C. Cell pellets were resuspended in 150 µl lysis buffer (50 mM Tris, pH 7.5, 150 mM NaCl, 0.1% Triton X-100, 10µg/ml aprotinin, 1µg/ml pepstatin, 0.5mM phenylmethylsulphonyl fluoride) and 10 µg protein from each strain was loaded onto a 12% pre-cast polyacrylamide gel (Biorad). Proteins were transferred to a nitrocellulose membrane (Biorad) with a Mini Trans-Blot Cell (Biorad) in transfer buffer containing 20 mM Tris, pH 8.3, 192 mM glycine, 20% (v/v) methanol and 0.1% (w/v) SDS. The membrane was blocked with 2% milk in phosphate-buffered saline (pH 7.4) with 0.1% Tween-20 (PBST) for 1 h and incubated for 2 h with primary anti-GFP (Rockland, 1:5,000 dilution) or anti-RecA (Abcam, 1:5000 dilution) antibody in blocking buffer. The membrane was then washed with PBST, incubated with secondary horseradish peroxidase conjugated goat anti-rabbit antibody (Rockland) at a dilution of 1:10,000 for 1 h and washed with PBST. Peroxidase was detected by SuperSignal West Pico Chemiluminescent Substrate (Pierce). Three biological replicates were performed for each strain tested. Band intensities were quantified with ImageJ software.

Gentle MAC extraction.
P. luteoviolacea was grown in 50 ml ASWT or NSWT media in 250 ml flasks at 30˚C and 200 rpm overnight (12-14 h). Cells were centrifuged for 20 min at 4000 g and 4˚C and resuspended in 5 ml cold extraction buffer (20 mM Tris, pH 7.5, 1M NaCl). Cultures were centrifuged for 20 min at 4000 g and 4˚C and the supernatant was isolated and centrifuged for 20 min at 6000 g and 4˚C. The supernatant fraction was isolated, in some cases treated with 500 µg/ml ampicillin for 1 h at 4˚C, and used for metamorphosis assays (100X dilution, derived from the equivalent of 10^7 cells/ml), electron microscopy, or bacteriocidal activity assays. Extracts were tested for viable cell contamination by plating 100 µl of extract on SWT agar and incubating overnight at room temperature.

Fluorescence microscopy.
P. luteoviolacea strains were cultured overnight (14-16 h) in ASWT media and spotted directly onto pads of 1% agarose in artificial seawater. Cells were immediately covered with a coverslip and imaged at room temperature. Fluorescence and phase contrast micrographs were captured using a Zeiss Axio Scope.A1, images were acquired with a Zeiss Axiocam MRm and processed using ImageJ software. For quantification of MAC-producer cells, *P. luteoviolacea* Δ*vipABhcp*Δ*bact2 macB-sfgfp* was grown for 10h (OD: 1.9), spotted onto a microscope slide and fluorescence/phase contrast images were captured with a Nikon Eclipse 90i microscope and a Photometrics CoolSNAP HQ^2 camera. Images were processed using ImageJ software. Timelapse microscopy was performed as described previously (*31*). *P. luteoviolacea macB-sfgfp* was cultured overnight in ASWT media, diluted 1:100 into fresh ASWT and spotted onto 1% low melting point agarose ASWT pads. Images were acquired every 10 minutes and fluorescent images were acquired with an exposure time of 500 ms.

Plunge freezing.
Copper/rhodium EM grids (R2/2, Quantifoil) were glow-discharged for 1 min. A 20×-concentrated bovine serum albumin-treated solution of 10 nm colloidal gold (Sigma) was added to a liquid culture (1:4 v/v) immediately before plunge freezing. A 4-µl droplet of the mixture was applied to the EM grid, then automatically blotted and plunge-frozen into a liquid ethane-propane mixture (*32*) using a Vitrobot (FEI Company) (*33*).

Electron cryotomography (ECT).
Images were collected using FEI Polara (at Caltech) or Titan (at HHMI Janelia Farm) 300kV FEG transmission electron microscopes equipped with energy filters (slit width 20 eV; Gatan) and 4 k×4 k K2 Summit direct electron detectors (Gatan). Pixels on the detector represented 0.48 nm (22,500×) or 0.32 nm (34,000×) at the Polara and 0.42 nm (26000x) at the Titan at the specimen level, respectively. Typically, tilt series were recorded from −60° to +60° with an increment of 1° and 10 µm under-focus. The cumulative dose of a tilt-series was 180–220 $e^-/Å^2$. UCSF Tomo (*34*) was used for automatic acquisition of tilt-series and 2D projection images. Three-dimensional reconstructions were calculated using the IMOD software package (*35*) or Raptor (*36*). 3dMOD (*35*) was used to visualize and segment tomograms, and to model repeating subvolumes. PEET (*37*) was used to align and average sub-volumes. Isosurface rendering was done in 3dMOD. 2D-slices through 3D-volumes were captured using 3dMOD. Sequential images were converted into movies using Quicktime Pro.

Negative-stain electron microscopy.
Samples were adsorbed to carbon-coated grids for 45 sec, washed with water and stained with 3% uranyl acetate for 45 sec. The grids were examined using a FEI T12 transmission electron microscope equipped with a 2kx2k CCD camera.

Mass spectrometry (MS) of purified bacteriocins.
Bacteriocins were prepared from *P. luteoviolacea* Δ*vipABhcp*Δ*bact2* mutant and *P. luteoviolacea* Δ*vipABhcp*Δ*bact2*Δ*macB*Δ*macS* mutant. Cells were cultured for 12-14 h at 30 ºC and 200 rpm in Bacto Marine Broth Medium (DIFCO 2216). Cultures were

harvested by centrifugation at 5,500 xg for 15 min at 4 ºC and the pellet was resuspended in 1.2 ml phosphate-buffered saline (10mM sodium phosphate, pH 7.4; 2.7 mM KCl; 137 mM NaCl). 750 µl of sample was transferred to a 15 ml tube and subjected to three rounds of sonication on ice (Misonix S-4000; amplitude 50; time 20 s; pulse "on" 1 s; pulse "off" 1 s). Intact cells and cell debris were removed by centrifugation at 16,000 xg for 5 min at 4 ºC. The supernatant containing the MACs was treated with 600 µl chloroform and 200 µl 2M NaCl and the sample was vortexed for 10 s. The sample was incubated standing at 20 ºC for 10 min, bacterial debris was removed by centrifugation at 10,000 xg for 30 min at 4 ºC. 1.4 ml of the aqueous supernatant was filter-sterilized through a 0.2 µm filter in a ultracentrifugation tube and centrifuged at 250,000 g for 90 min at 4ºC. The pellet was resuspended in 300 µl marine broth and treated with DNaseI (5 µg/ml) and RNaseA (1 µg/ml). The sample was incubated standing at 20 ºC for 10 min and subsequently centrifuged at 12,000 g for 10 min at 4ºC. The supernatant was applied to 2 ml of 40% glycerol in marine broth and centrifuged at 250,000 g for 90 min at 4ºC. The pellet was resuspended in 300 µl extraction buffer (20 mM Tris buffer, pH 7.5; 1 M NaCl). The supernatant was again applied to 2 ml of 40% glycerol in marine broth and centrifuged at 250,000 g for 90 min at 4ºC. After adding 2 ml extraction buffer and gently resuspending the pellet, the sample was centrifuged at 200,000 g for 90 min. The centrifugation tubes were inverted on paper towels for 10 min. The pellet was resuspended in 200 µl extraction buffer. Bands were cut out after running the sample on a 12% SDS-PAGE and analyzed by MS to identify peptides (Protein/Peptide Micro Analytical Laboratory, Caltech).

Genomics and phylogenetic analysis.

To reconstruct phylogenetic trees, sequences of protein domains from MacT1 (aa 3-132), MacT2 (aa 6-146), Afp1 (aa 16-144), Afp5 (aa 7-142), PAU_02790 (aa 16-144), PAU_02794 (17-145), CAHE_0461 (aa 9-144) and Aasi_1077 (aa 10-145) were combined with the full set of reference sequences from Pfam protein families PF06841 (*38*) and a profile hidden Markov model was produced from the sequences using hmmbuild (hmmer.org). All protein domain sequences in the National Center for Biotechnology (NCBI) non-redundant database matching the profile were then acquired using hmmsearch (*39*) using sequence and hit e-values of 0.01 and 0.03, respectively. Sequences were clustered using CD-HIT (*40*) with a sequence identity cutoff value of 0.3. Sequences were then realigned and trimmed with hmmalign (hmmer.org). The best model of amino acid replacement was determined to be LG+G+F with ProtTest 2.4 (*41*), and phylogenies were constructed with PhyML version 3.0 (*42*) where branching support was calculated using the approximate likelihood ratio test (aLRT) with SH-like interpretation (*29*). Final trees were rendered using iTOL (*43*) and Adobe illustrator.

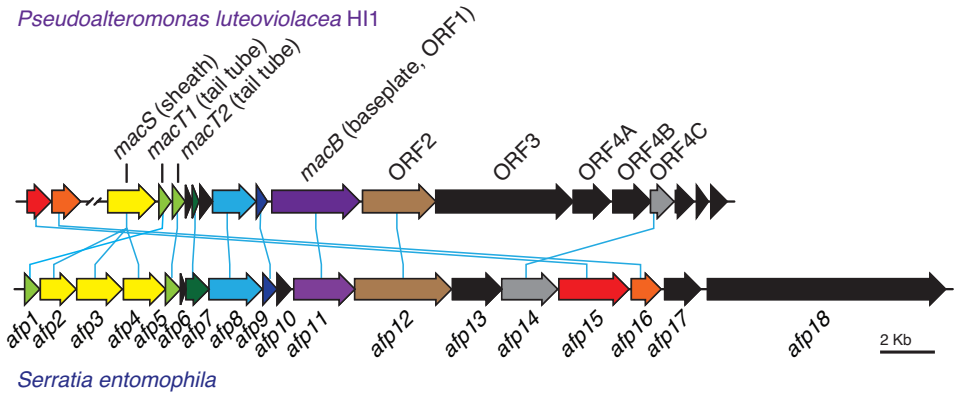

Fig. S1. *P. luteoviolacea mac* gene cluster and synteny with *S. entomophila afp* gene cluster.

Genes identified by Huang *et al.* (7) are indicated as ORF1, ORF2, ORF3 and ORF4A/B/C. ORF4 was determined to consist of 3 ORFs.

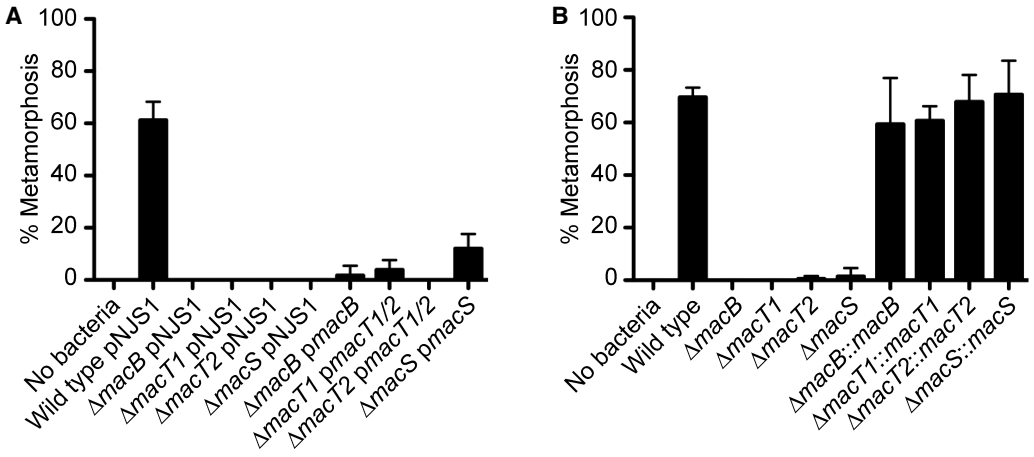

Fig. S2. Complementation and gene replacements of *mac* mutant strains.

(A) Metamorphosis (%) of *H. elegans* in response to biofilms of *P. luteoviolacea* wild type, Δ*macB*, Δ*macT1*, Δ*macT2*, Δ*macS* containing pNJS1, p*macB*, p*macT1/2* or p*macS*. Strains were grown in the presence of 200 µg/mL kanamycin to maintain plasmids. **(B)** Metamorphosis (%) of *H. elegans* in response to biofilms of *P. luteoviolacea* wild type, Δ*macB*, Δ*macT1*, Δ*macT2*, Δ*macS* or strains where the in-frame gene deletion was restored with the wild-type gene (Δ*macB::macB*, Δ*macT1::macT1*, Δ*macT2::macT2*, Δ*macS::macS*). Sterile artificial seawater (no bacteria) was used as a negative control. Error bars represent standard deviations (n=5).

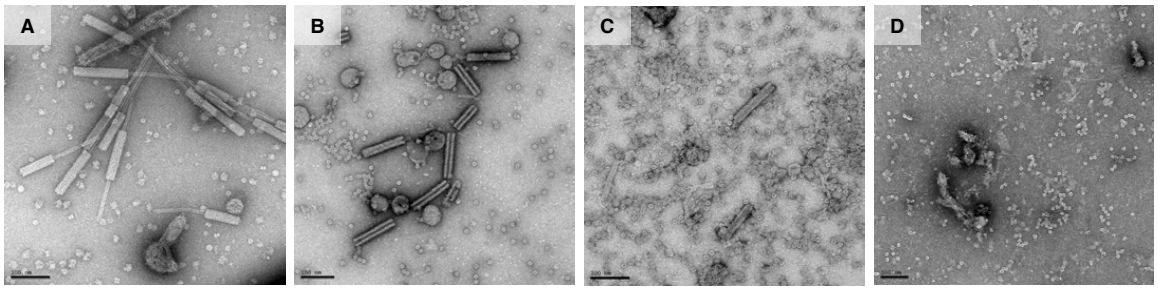

Fig. S3. Negative stain electron micrographs of bacteriocin purifications of different *P. luteoviolacea* mutants.

(A-D) Negative stain EM of bacteriocin purifications from *P. luteoviolacea* (A) wild type, (B) Δ*vipABhcp*Δ*bact2*, (C) Δ*vipABhcp*Δ*macS*Δ*macB* and (D) Δ*vipABhcp*Δ*bact2*Δ*macS*Δ*macB*. No sheaths or phage tail-like bacteriocins were observed in D. Bars, 100 nm.

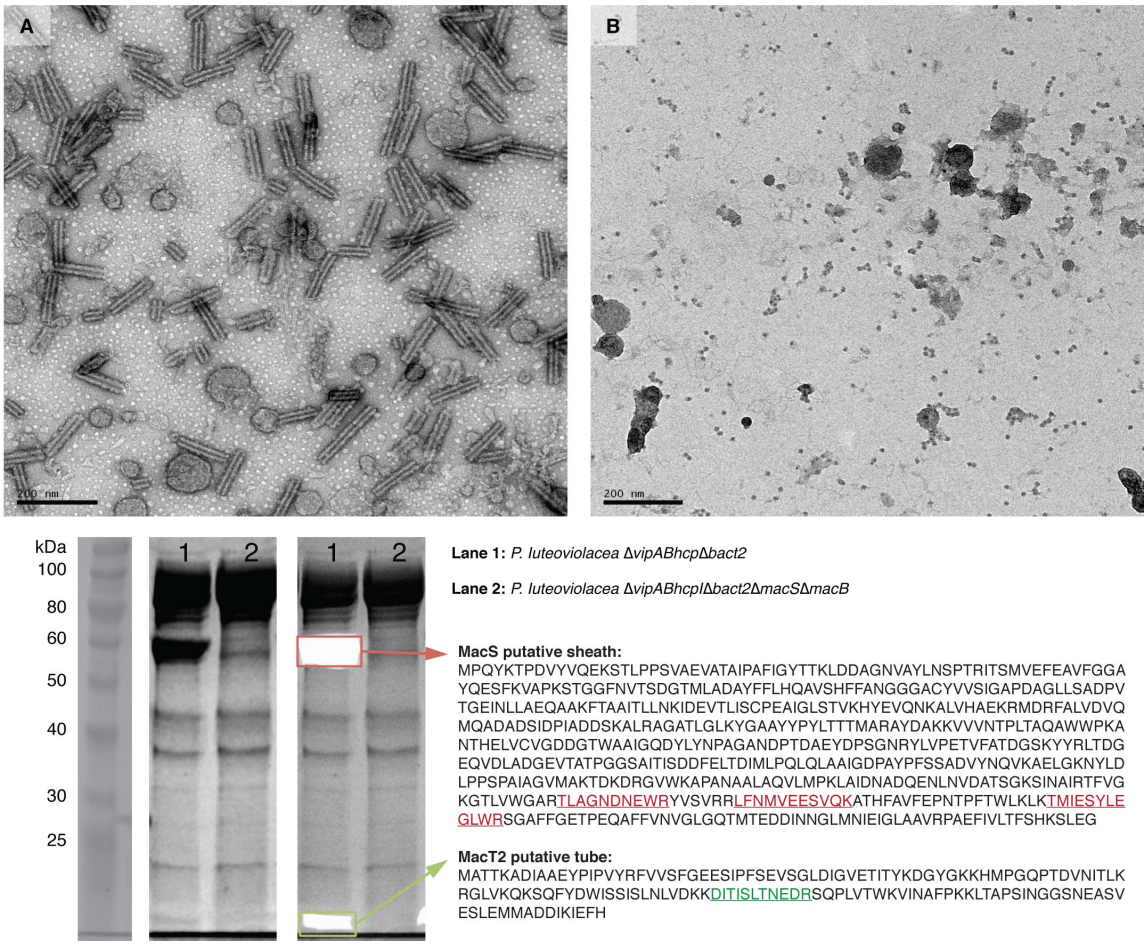

Fig. S4. Identification of Mac proteins in bacteriocin purifications.

Negative stain EM of a bacteriocin purification from **(A)** *P. luteoviolacea* Δ*vipABhcp*Δ*bact2* and **(B)** *P. luteoviolacea* Δ*vipABhcp*Δ*bact2*Δ*macS*Δ*macB*. **(C)** SDS-PAGE of the purifications from (lane 1) *P. luteoviolacea* Δ*vipABhcp*Δ*bact2* and (lane 2) *P. luteoviolacea* Δ*vipABhcp*Δ*bact2*Δ*macS*Δ*macB***.** Two bands present in lane 1 but lacking in lane 2 were subjected to mass spectrometry and identified as MacS and MacT2. Identified peptides are underlined. Note that the expected molecular weights of MacS (62 kDa) and MacT2 (17 kDa) match the height of the analyzed bands. Bars, 200 nm.

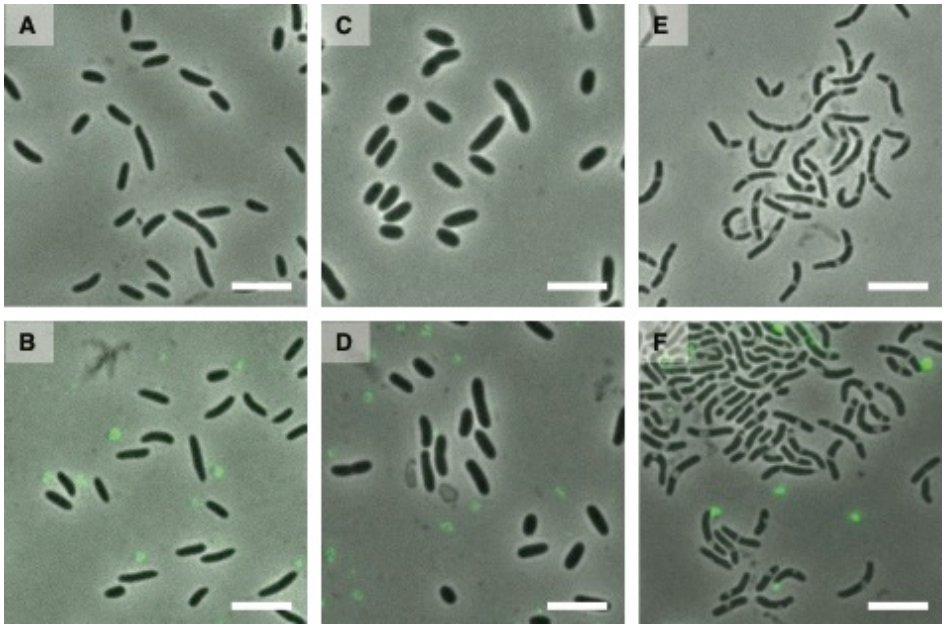

Fig. S5. MacB-sfGFP expression in three marine media.

(A-F) Merged phase contrast and fluorescence micrographs of *P. luteoviolacea* wild-type (A, C, E) and *macB-sfgfp* (B, D, F) strains grown overnight in ASWT (A, B), NSWT (C, D) and 2216 (E, F) media. Scale bars, 5 μm.

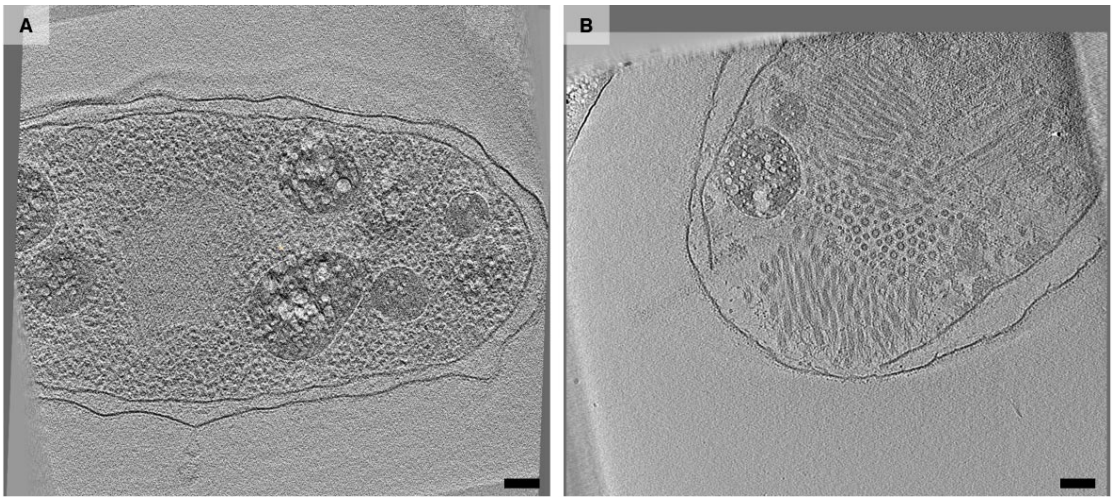

Fig. S6. Examples of *P. luteoviolacea* cells imaged by ECT.

(A) ECT of an intact *P. luteoviolacea* Δ*vipABhcp*Δ*bact2* cell that is not producing MACs. **(B)** ECT of a *P. luteoviolacea* Δ*vipABhcp*Δ*bact2* cell producing MACs. The membrane morphology (no cytoplasmic membrane at the pole) indicates that the cell is in the process of lysis. Shown are 19.7 nm thick slices. Bars, 100 nm.

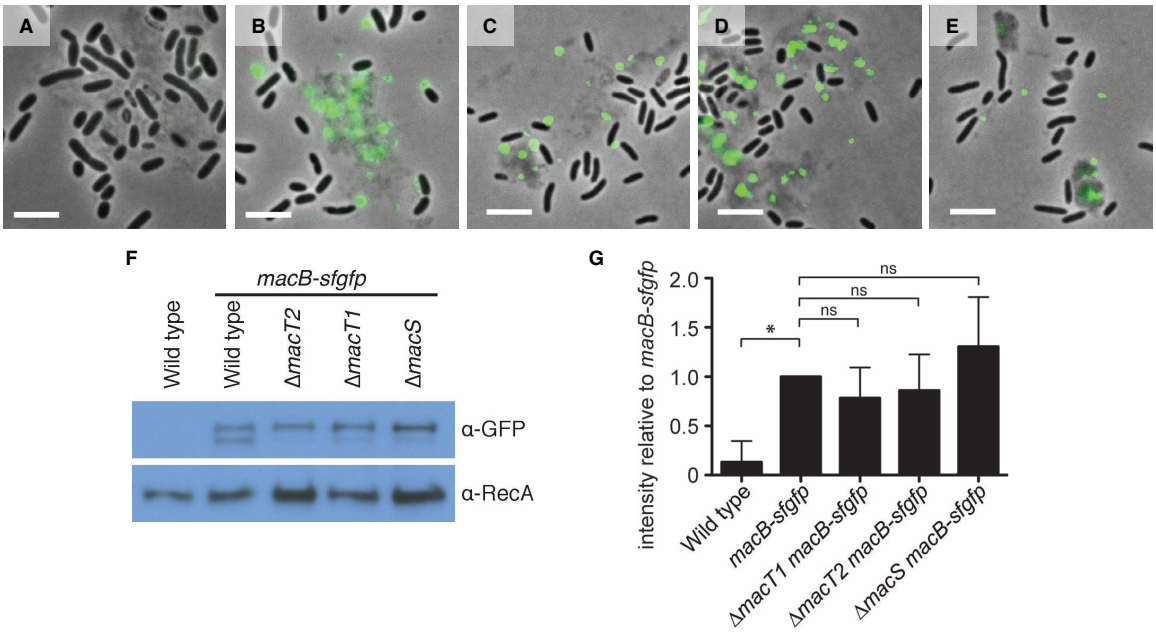

Fig. S7. MacB-sfGFP production in wild-type and *mac* mutant strains.

(A-E) Micrographs of merged phase-contrast and fluorescence images of *P. luteoviolacea* wild-type (A), *macB-sfgfp* (B), Δ*macS macB-sfgfp* (C), Δ*macT1 macB-sfgfp* (D) and Δ*macT2 macB-sfgfp* (E) strains. Bar, 5 µm. **(F)** Immunoblot of *P. luteoviolacea* strains with anti-GFP and anti-RecA antibodies. One representative immunoblot of three biological replicates is shown. **(G)** Quantification of anti-GFP immunoblot of *P. luteoviolacea* wild-type, *macB-sfgfp*, Δ*macS macB-sfgfp*, Δ*macT1 macB-sfgfp* and Δ*macT2 macB-sfgfp* strains relative to *macB-sfgfp*. Error bars indicate standard deviations of 3 biological replicates. Data were analyzed by Student's t-test: *p < 0.05; not significant (ns).

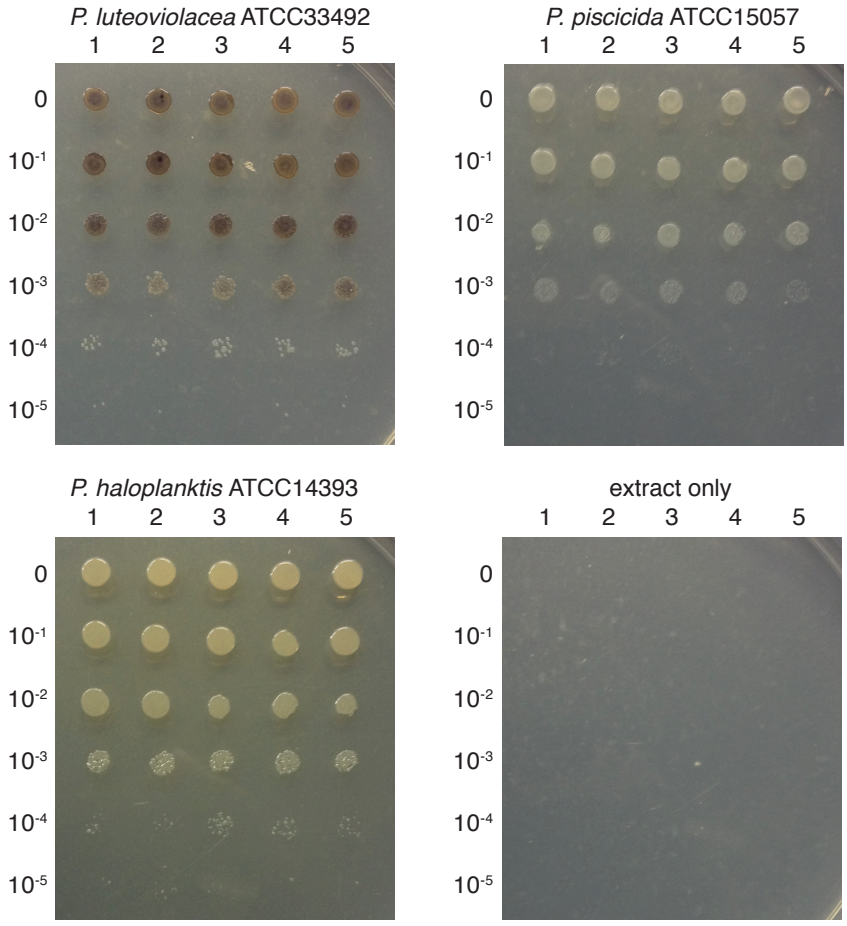

Fig. S8. MACs do not possess bacteriocidal activity against other *Pseudoalteromonas* species.

Activity assay of extracts from *P. luteoviolacea* wild-type (2), Δ*vipABhcp*Δ*bact2* (3), Δ*vipABhcp*Δ*macS*Δ*macB* (4) and Δ*vipABhcp*Δ*bact2*Δ*macS*Δ*macB* (5) strains against *P. luteoviolacea* ATCC 33492, *P. piscicida* and *P. haloplanktis* cultures. Liquid overnight cultures of each indicator strain were mixed with extracts (10X dilution), incubated for 1 h at 25˚C and 10-fold serial dilutions were spotted onto ASWT or 2216 agar plates. Buffer alone (1) and extract only without indicator strain were used as controls.

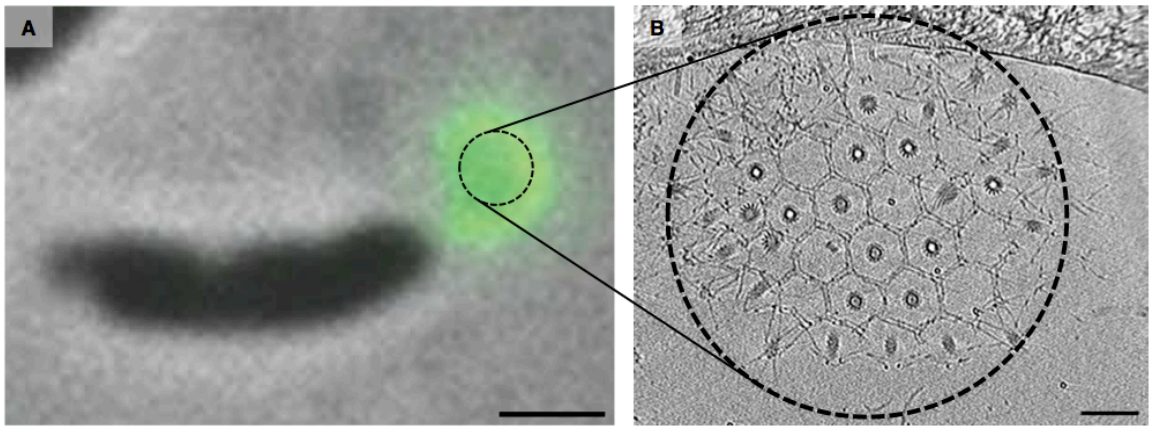

Fig. S9. Matching dimensions of MAC arrays imaged by fluorescence light microscopy and ECT.

(A) Fluorescence image of an extracellular MAC array. Bar, 1000 nm. **(B)** ECT of MAC outside cell. Circles indicates an array with a diameter of 700 nm. Bar, 100 nm.

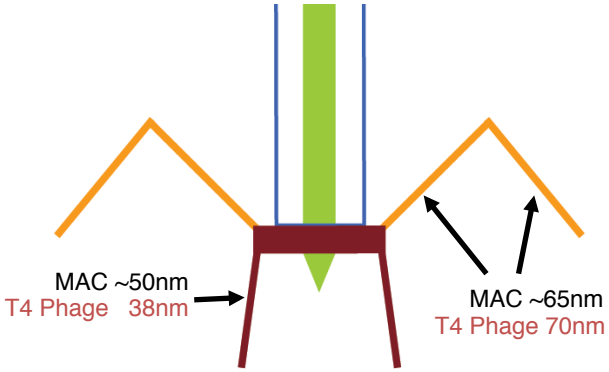

Fig. S10. Comparison of phage and MAC tail fiber dimensions.

Schematic of a phage tail-like structure. Length values of tail fibers as well as length ratios match tail fibers observed in T4 phage and MAC.

Table S1. ORFs in the *mac*, *bact2* or T6SS locus and translated protein homology.

ORF	Pfam no. (e-value)	Pfam domain	Predicted function	Afp homolog (Identity/e-value)
Afp15 homolog	PF00004 (2.3e-27)	AAA	ATPase	Afp15 (35%/6e-50)
Afp16 homolog	DUF4255 (5.8e-16)			Afp16 (31%/7e-05)
macS	PF04984 (4.8e-28)	Phage_sheath_1	Phage tail sheath	Afp2 (53%/1e-60), Afp3 (51%/4e-59), Afp4 (44%/5e-48)
macT1	PF06841 (2.1e-32)	Phage_T4_gp19	Phage tail tube	Afp1 (52%/2e-54), Afp5 (23%/3e-12)
macT2	PF06841 (3.1e-13)	Phage_T4_gp19	Phage tail tube	Afp5 (33%/3e-20), Afp1 (26%/2e-09)
Afp7 homolog	No similarity			Afp7 (27%, 3e-06)
Afp8 homolog	PF04717 (3e-07)	Phage_base_V	Phage tail spike	Afp8 (24%, 2e-24)
Afp9 homolog	PF04965 (1.3e-13)	GPW_gp25	lysozyme	Afp9 (42%, 6e-20)
macB	PF04865 (9.4e-03)	Baseplate_J	Phage baseplate	Afp11 (45%, 3e-14)
Afp12 homolog	No similarity			Afp12 (71%, 3e-15)
Afp14 homolog	No similarity			Afp14 (36%, 2e-09)
bact2 tube	PF04985 (4.9e-46)	Phage_tube	Phage tail tube	
bact2 sheath	PF04984 (3.4e-55)	Phage_sheath_1	Phage tail sheath	
vipA	DUF770 (2.4e-47)		T6SS VipA	
vipB	DUF877 (2.7e-175)		T6SS VipB	
hcp	DUF796 (5.5e-39)		T6SS Hcp	

Table S2. ECT measurements of MACs and MAC arrays.

Structure measured (reference to figure)	Average measurement +/- SD
MAC array in X (Fig. 3B-I)	715-773 nm
MAC array in Y (Fig. 3B-I)	870-922 nm
MAC array in Z (Fig. 3B-I)	330 nm
Intracellular sheath spacing in plane of baseplate (Fig. 3A)	41 nm +/- 7nm, n=42
Extracellular sheath spacing in plane of hexagonal net (Fig. 3E)	97 nm +/- 6nm, n=108
Extended sheath length (Fig. 4B)	314 nm +/- 13 nm, n=70
Contracted sheath length (Fig 4B, C)	148 nm +/- 6 nm, n=6
Contracted sheath with jammed tube length (Fig 4D)	147 nm +/- 5nm, n=5
Extended sheath diameter (Fig. 4B)	13 nm
Contracted sheath diameter (Fig 4F)	16 nm
Inner tube diameter (Fig 4K)	7 nm

Table S3. Strains and plasmids used in this work.

Strain or Plasmid	Genotype	Source or Reference
***Pseudoalteromonas* strains**		
HI1	*P. luteoviolacea* HI1	(*8*)
HI1 Str^R	*P. luteoviolacea* HI1, wild type	(*7*)
Δ*macB*	*P. luteoviolacea* HI1 Δ*macB*, Str^R	This study
Δ*macT2*	*P. luteoviolacea* HI1 Δ*macT2*, Str^R	This study
Δ*macT1*	*P. luteoviolacea* HI1 Δ*macT1*, Str^R	This study
Δ*macS*	*P. luteoviolacea* HI1 Δ*macS*, Str^R	This study
Δ*vipABhcp*	*P. luteoviolacea* HI1 Δ*vipABhcp*, Str^R	This study
Δ*bact2*	*P. luteoviolacea* HI1 Δ*bact2*, Str^R	This study
Δ*vipABhcp* Δ*bact2*	*P. luteoviolacea* HI1 Δ*vipABhcp* Δ*bact2*, Str^R	This study
Δ*vipABhcp* Δ*macB*	*P. luteoviolacea* HI1 Δ*vipABhcp* Δ*macB* Str^R	This study
Δ*vipABhcp* Δ*macB* Δ*macS*	*P. luteoviolacea* HI1 Δ*vipABhcp* Δ*macB* Δ*macS*, Str^R	This study
Δ*vipABhcp* Δ*bact2* Δ*macB* Δ*macS*	*P. luteoviolacea* HI1 Δ*vipABhcp* Δ*bact2* Δ*macB* Δ*macS*, Str^R	This study
macB-sfgfp	*P. luteoviolacea* HI1 *macB-sfgfp*, Str^R	This study
Δ*macS macB-sfgfp*	*P. luteoviolacea* HI1 Δ*macS macB-sfgfp*, Str^R	This study
Δ*macT1 macB-sfgfp*	*P. luteoviolacea* HI1 Δ*macT1 macB-sfgfp*, Str^R	This study
Δ*macT2 macB-sfgfp*	*P. luteoviolacea* HI1 Δ*macT2 macB-sfgfp*, Str^R	This study
ATCC 33492	*P. luteoviolacea*, ATCC strain 33492	(*44*)
ATCC 14393	*P. haloplanktis*, ATCC strain 14393	(*45*)
ATCC 15057	*P. piscicida*, ATCC strain 15057	(*45*)
Plasmids		
pCVD443	pGP704 derivative, *mob/oriT sacB*, Ap^R, Km^R	(*7*)
pΔ*macB*	pCVD443::Δ*macB*, Ap^R, Km^R	This study
pΔ*macT2*	pCVD443::Δ*macT2*, Ap^R, Km^R	This study
pΔ*macT1*	pCVD443::Δ*macT1*, Ap^R, Km^R	This study
pΔ*macS*	pCVD443::Δ*macS*, Ap^R, Km^R	This study
p*macB*	pCVD443::*macB*, Ap^R, Km^R	This study
p*macS/T1/T2*	pCVD443::*macS/T1/T2*, Ap^R, Km^R	This study
pΔ*vipABhcp*	pCVD443::Δ*vipABhcp*, Ap^R, Km^R	This study
pΔ*bact2*	pCVD443::Δ*bact2*, Ap^R, Km^R	This study
p*macB-sfgfp*	pCVD443::*macB-sfgfp*, Ap^R, Km^R	This study
pANT3	*ori*RSF1010 *mob* Km^R Str^R, promoterless *gfpmut3*	(*46*)
pNJS1	pANT3 Δ*gfpmut3*	This study
p*macB*	pNJS1::*macB*	This study
p*macT1/2*	pNJS1::*macT1 macT2*	This study
p*macS*	pNJS1::*macS*	This study

Table S4. Primers used in this work.

Primer	Sequence
*macB*_dA	GGTCGACGGATCCCAAGCTTCTTCTAGAGGTACCGCATGCAACCCAGACACTGAGGTGCT
*macB*_dB	TTTCCATTTTCCAATCCCTTCGCCAGAGATAAGTGATTGACTACGA
*macB*_dC	TCGTAGTCAATCACTTATCTCTGGCGAAGGGATTGGAAAATGGAAA
*macB*_dD	ACACAACGTGAATTCAAAGGGAGAGCTCGATATCGCATGCCATAACCTGGCTGAGCACCT
*macT2*_dA	GGTCGACGGATCCCAAGCTTCTTCTAGAGGTACCGCATGCCTCGTACGCTAGCGGGTAAC
*macT2*_dB	ATAGGCACAGCCACCAAATCCATGGGAGTTCTAGGGTCTTGA
*macT2*_dC	TCAAGACCCTAGAACTCCCATGGATTTGGTGGCTGTGCCTAT
*macT2*_dD	TTTTGAGACACAACGTGAATTCAAAGGGAGAGCTCGCTCCAATGGTGGGTAGGTA
*macT1*_dA	GGTCGACGGATCCCAAGCTTCTTCTAGAGGTACCGCATGCCGGTGAAGTAACAGCGACAC
*macT1*_dB	AATCTTGATGTCATCTGCCATTGCTGCGATATCTGCTTTAGT
*macT1*_dC	ACTAAAGCAGATATCGCAGCAATGGCAGATGACATCAAGATT
*macT1*_dD	TTTTGAGACACAACGTGAATTCAAAGGGAGAGCTCATCGCCACGCTCAATTTTT
*macS*_dA	GGTCGACGGATCCCAAGCTTCTTCTAGAGGTACCGCATGCGAGGGGCCGAGTTATACGTT
*macS*_dB	GCAAGAATTAACCTTCAAGGCTGACGTAGACGTCTGGGGTTT
*macS*_dC	AAACCCCAGACGTCTACGTCAGCCTTGAAGGTTAATTCTTGC
*macS*_dD	TTTTGAGACACAACGTGAATTCAAAGGGAGAGCTCTCCCATTCCCAGCTTTCTAA
vipABhcp_dA	GGTCGACGGATCCCAAGCTTCTTCTAGAGGTACCGCATGCGGTACCGCCTAAGGTGACAA
vipABhcp_dB	ACGACCCTCAGTCCAAGAATCCGCTCTGGGTATTTCTTTTTGA
vipABhcp_dC	TCAAAAAGAAATACCCAGAGCGGATTCTTGGACTGAGGGTCGT
vipABhcp_dD	TTTTGAGACACAACGTGAATTCAAAGGGAGAGCTCAACTTAATTTGGCGCCACTG
bact2_dA	GGTCGACGGATCCCAAGCTTCTTCTAGAGGTACCGCATGCTTCAGCAATCAAAGCACAGG
bact2_dB	TTAAGCTCCGATAGTCTTGCGACCGTGTAGAAATCCCGACAT
bact2_dC	ATGTCGGGATTTCTACACGGTCGCAAGACTATCGGAGCTTAA
bact2_dD	TTTTGAGACACAACGTGAATTCAAAGGGAGAGCTCTTCAGTGTCTCGGCTTGTTG
macB-sfGFP_A	ATTGGCGGCGCCAAAGCCCACTTCACCGGGGATCCTTACGGTTCCTGGCCTTTT
macB-sfGFP_B	GCTCTTCGCCTTTACGCATTCCGCCACCTGCCGCAGCTTGCACAACAAAATTATGCTGA
macB-sfGFP_C	TCAGCATAATTTTGTTGTGCAAGCTGCGGCAGGTGGCGGAATGCGTAAAGGCGAAGAGC
macB-sfGFP_D	CGTCGCTTTAAATGTAAGTAGCTTATTTGTACAGTTCATCCATACCAT
macB-sfGFP_E	ATGGTATGGATGAACTGTACAAATAAGCTACTTACATTTAAAGCGACG
macB-sfGFP_F	TTTTGAGACACAACGTGAATTCAAAGGGAGAGCTCGCTTCTTAACCGGTGTGCTC
pANT3_gbsnF	GGATCCCCGGTGAAGTGG
pANT3_gbsnR	CGTGAAGAAGGTGTTGCTGA
pNJS_*macB*_F	TTGGCGGCGCCAAAGCCCACTTCACCGGGGATCCTCAGGGCCTGATATGGAAGACGGAGA
pNJS_*macB*_R	GCAGACCTCAGCGCCCCCCCCCCCCCTGCAGAGATGACGCCAAACCTTCAA
pNJS_*macT1/2*_F	ATTGGCGGCGCCAAAGCCCACTTCACCGGGGATCCGGAACGCTTGTTTGGGGTGC
pNJS_*macT1/2*_R	GCAGACCTCAGCGCCCCCCCCCCCCCTGCAGTCCTTACACTGGCACACCTG
pNJS_*macS*_F	TTGGCGGCGCCAAAGCCCACTTCACCGGGGATCCCAAGTGAATTTGTCAATCACTCAAAT
pNJS_*macS*_R	GCAGACCTCAGCGCCCCCCCCCCCCCTGCAGCATGGTTCAGCGCCAAATAG

Movie S1. Timelapse of *P. luteoviolacea macB-sfgfp*.

Live cell imaging of a culture on an agarose pad. Images were recorded every 10 min. sfGFP signal is shown in green. A lysing cell is indicated by the arrow.

Movie S2. Two tomograms of MACs inside cells.

Slices through electron cryotomograms of two MAC-containing cells are shown.

Movie S3. Tomogram and model of a MAC array.

Slices through an electron cryotomogram of the MAC array in Fig. 3B-G and different perspectives of the corresponding model in Fig. 3H, I.

Movie S4. Two tomograms with several MACs.

Slices through electron cryotomograms of different MAC arrays.

Movie S5. Tomogram showing differences between contracted and extended conformation.

Slices through an electron cryotomogram from yet another orientation of the MAC array in Fig. 3B-G.

Movie S6. Surface rendering of a subtomogram average of a MAC in extended conformation.

Slices through a subtomogram average of extended MACs (longitudinal and perpendicular orientations) and different perspectives of the corresponding surface rendering. Color code is the same as in Fig. 4.

Movie S7. Surface rendering of a subtomogram average of a MAC in contracted conformation.

Slices through a subtomogram average of contracted MACs (perpendicular orientation) and different perspectives of the corresponding surface rendering. Color code is the same as in Fig. 4.

Movie S8. Surface rendering of a subtomogram average of MAC net vertices.

Slices through a subtomogram average of the hexagonal net vertices and different perspectives of the corresponding surface rendering. Color code is the same as in Fig. 4.